ARTIGO ORIGINAL

REVISTA CEREUS
ISSN: 2175-7275

3D reconstruction method applied to sediment layers in computed tomography geometry

Método de reconstrução 3D aplicados a camadas de sedimentos em geometria de tomografia computadorizada

Joel Sánchez Domínguez[1], Gabriela Hoff[2], Joaquim Teixeira de Assis[3], Antonio Brunetti[4], Susana Marrero Iglesias[5]

RESUMO

A obtenção de informações sobre o depósito de sedimentos é uma tarefa difícil devida à fragilidade do meio analisado. A utilização de testes não destrutivos para produzir dados confiáveis nesses ambientes está sendo avaliada por vários pesquisadores. O presente estudo propõe a avaliação da geometria de irradiação de tomografia computadorizada (TC) para obtenção de imagens das camadas de testemunhos de sedimentos. Num primeiro estágio, imagens planares de objetos geométricos em geometria centrada, similar a utilizada em processos de tomografia computadorizada, foram simuladas usando o código dedicado X-Ray Monte Carlo (XRMC). Posteriormente as radiografias foram processadas usando o algoritmo de reconstrução Feldkamp, David e Kress (FDK) para gerar o volume tridimensional. O método FDK foi avaliado para reconstrução de imagens definidas com 8 e 64 bits de cores. O método de reconstrução apresentou-se adequado para reconstruir imagens usando 64 bits na escala de cinza mostrando uma exatidão nas medidas dos objetos de contraste com desvios máximos de 8%. Artefatos de imagens, vantagens e desvantagens do método de reconstrução para o caso avaliado são abordados nesse artigo. Os resultados obtidos mostram a possibilidade de aplicação da metodologia para produzir imagens detalhadas de testemunhos de sedimentos coletados em lagos, rios ou tanques de simulação de deposição.

Palavras-chave: Tomografia Computadorizada. XRMC. Algoritmo FDK. Imageamento de Sedimentos.

[1] Doutor em Modelagem Computacional pelo IPRJ/UERJ.

Instituto Politécnico Universidade do Estado do Rio de Janeiro

https://orcid.org/0000-0003-4330-8593

E-mail: jsdominguez@iprj;uerj.br

[2] Doutora em Biociências Nucleares pela UERJ

Instituto Nazionale di Fisica Nucleare (INFN) - Sezioni di GE

https://orcid.org/0000-0002-7460-8030

[3] Doutor em Engenharia Nuclear pela UFRJ.

Instituto Politécnico Universidade do Estado do Rio de Janeiro

https://orcid.org/0000-0002-4027-6939

[4] Doutor em Física Médica pela USP.

University of Sassari, Italy

https://orcid.org/0000-0002-0116-1899

[5] Doutora em Modelagem Computacional pelo IPRJ/UERJ.

Universidade Estadual de Santa Cruz, Ilhéus Bahia.

https://orcid.org/0000-0002-4955-6216

ABSTRACT

Obtaining information on sediment deposition is a difficult task due to the fragility of the analyzed medium. The use of non-destructive tests to produce reliable data in these environments is being evaluated by some researchers. The current study proposes the computed tomography (CT) irradiation geometry evaluation, for obtaining images of the sediment deposition layers. As a first stage, planar images of geometric objects in centered geometry, similar to those resulting from the CT processes, were simulated using the dedicated X-Ray Monte Carlo (XRMC) code. Then, the x-rays were processed using the Feldkamp, David and Kress (FDK) reconstruction algorithm to generate the three-dimensional volume. Evaluating the FDK method for the reconstruction of the 8 to 64 color bits images, the obtained results were satisfactory for 64 bits grayscale images. The method showed accuracy in the contrast objects measurements, presenting a maximum deviation of 8%. This article discusses the constructed image artifacts and also, the advantages and disadvantages of the reconstruction method. The results show the feasibility of applying the methodology to produce detailed images of sediment samples collected in lakes, rivers or deposition simulation tanks.

Keywords: Computed Tomography. XRMC. FDK Algorithm. Sediments Imaging.

1. INTRODUCTION

The characterization of regions using the computational simulation of the sediment deposition process is widely used in geological studies (MIALL, 2006; BJORLYKKE, 2015). Nevertheless, as a result of the sediment deposition structures fragility, its evaluation must be done through minimally invasive or non-invasive methods. This kind of methods avoids destroying information from the unstable and delicate structure.

Computed tomography (CT) is a non-destructive test that allows to obtain images of the axial sections from a set of an object x-rays (DOMINGUEZ, 2016). The transmission and processing information about the planar images generate a stack of cutaway images of the object. The internal structures can be characterized by the shade of gray and position. CT is a widely accepted technology with numerous applications in medicine, industry and scientific research (DOMINGUEZ, 2016).

The present study proposes to explore the 3D Feldkamp, David and Kress (FDK) reconstruction method for the evaluation of collected sediment samples. These samples are designed according the data collection geometry used in CT to obtain images of sediment layers. The FDK reconstruction algorithm is a filtered back-projection algorithm for tomographic images 3D reconstruction (DOMINGUEZ, 2016). In order to evaluate the reconstruction method, it was used planar images generated by simulation with the X-Ray Monte Carlo software (XRMC) considering radiographic images generated in a similar geometry to those obtained using a CT equipment. In the following section we briefly discuss some characteristics of CT, the reconstruction method and the XRMC package. In section 3 we describe the methodology applied, including the data preparation and the application of the reconstruction model. In section 4 we present the preliminary results for the created images. Finally, we present the conclusions and the next steps in this research.

2. COMPUTED TOMOGRAPHY AND THE RECONSTRUCTION METHOD

CT can be analyzed as a two-step process: the exploration of the samples through the planar images generation and the axial cuts images reconstruction. Generally, in the exploration step, a source/detector set is used to irradiate the studied object in different angles, detecting the radiation amount that passes through the object (transmission study). The result of this process are, flat images, for every irradiated angle. This set of images can be obtained rotating the source/detector set around the body or otherwise by the object

rotation in front of the emission source. The simulation process performed in this work to obtain the planar images emulates the scanning, in which the object rotates and the source/detector set is fixed. This type of exploration is similar to the irradiation geometry in CT equipment for research and industrial applications due to its lower mechanical complexity.

In the 3D reconstruction step of the CT process, a computational algorithm calculates every planar image´s contribution for each volume point to be reconstructed. In this work, the FDK algorithm (FELDKAMP et al., 1984) was used to do the reconstruction. The FDK is an analytical reconstruction algorithm for cone beam, which has been the basis of the most commonly used algorithms (KALENDER, 2011). The formulation is only valid for circular trajectories of the radiation source. Variations of the algorithm were developed for helical trajectories (OLIVEIRA, 2002). Equation 1 shows how the FDK algorithm calculates density f(r) as a function of the filtered projections PΦ(Y,Z) from planar images. The subscripts i, r, k reflects the discretization of these projections. Further details regarding the algorithm mathematical basics can be consulted in (DOMINGUEZ, 2016) and (FELDKAMP et al., 1984).

$$f(\vec{r}) = \frac{1}{4\pi^2} \sum_i \Delta\Phi \frac{d^2}{(d + \vec{r} \cdot \hat{x}')^2} \tilde{P}_{\Phi i}(Y_r, Z_k)$$

(1)

After axial planes reconstruction, the images can be stacked to visualize the volume as a whole. The rendered volume can be manipulated with imaging tools to produce lateral or sagittal plane images, and also, frontal or coronal planes.

The reason of the selection of the FDK algorithm in this work to perform the reconstruction is that being an analytical algorithm its performance (time and processing) is better when compared with other algorithms as the iterative ones. On the other hand, it produces excellent results in different CT applications (KALENDER, 2011). However, it has some limitations such the raising of computational cost when the image quality increases (SHUNLI et al,.2018) and also the algorithm need a full exploration of the object (360º images) to performs the study. These characteristics complicate its use for on-site studies and real geometries (rivers, lakes and / or simulation tanks) when only some section's radiographies are available for analysis. Nevertheless, for a sample study (geological evidences), this method is a good alternative.

2.1. COMPUTATIONAL IMPLEMENTATION OF THE FDK ALGORITHM

To implement the FDK reconstruction algorithm, a C ++ program was developed. The program input data included:

a) number of projections;

b) width and height of images projection;

c) images projections;

d)reconstruction initial and final plane.

The program output is a RAW file containing the reconstructed image, a volume with a square base with a side equal to the width of the image projections and a depth equal to the number of the reconstructed planes, the difference between the final and initial planes of the reconstruction. The RAW format is used for digital images and contains all the available image data. This format is used in TC to store images complete sequence obtained from the sample exploration. Figure 2 shows the implemented program flow diagram to execute the reconstruction process.
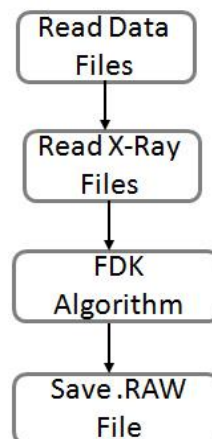

Figure 1. Software routine flow diagram developed for reconstruction process.

In this implementation, a background image (no object present) is used to compare the maximum radiation at the detector with and without the sample. In 8-bit color images, this background image had a fixed value in all of its pixels, however, using 64-bit color images

DOI: 10.18605/2175-7275/cereus.v13n3p68-82
Revista Cereus
2021 Vol. 13. N.3

DOMINGUEZ, J.S; HOFF, G; DE ASSIS, J.T; BRUNETTI, A; IGLESIAS, S.M
3D reconstruction method applied to sediment layers in computed tomography geometry

the fixed value in the background image produces distortions in the planar images. For that reason, it was necessary to create a simulated background, an x-ray generated in the same geometry but without the object. In the reconstruction final stage, a normalization of the pixels in the volume was made using the images grayscale limits. In the 8-bit images these limits were fixed from 0 to 256 but in 64-bit images, the maximum and minimum values produced during the reconstruction were used, generating a better visualization of the low contrast images.

3. SOFTWARE X RAY MONTE CARLO

The XRMC is a dedicated Monte Carlo code for precise simulation of images generated by X-ray transmission and spectroscopy experiments in heterogeneous samples. The use of the Monte Carlo method makes the code suitable for detailed simulation of complex experiments in generic samples. The program is written in C ++ and has been tested on Linux, Mac OS X and MS Windows platforms. The software package is being developed by the University of Sassari researchers and is available for the scientific community use under a general GNU license (GOLOSIO et al., 2013).

Approximations of the Monte Carlo method are often used to simulate the particles interactions with the matter, under different experimental conditions. However, these methods applied to X-ray imaging and spectroscopy experiments require a high computational effort. Also, have some other limitations such as the inclusion of a limited region of the space or photons produced by rare interaction in the final channels. To solve these problems, the XRMC combines the Monte Carlo method with variance reduction techniques, reducing by several orders the simulation times (OLIVA et al., 2015).

Several XRMC applications have been reported in the literature recently as (HOFF et al., 2017; MANSO et al., 2015; BRUNETTI et al., 2016; HOFF et al., 2010). XRMC has a user-friendly interface, with scripts to determine the devices that describe the geometry, material, quantities to be simulated, and final results output format.

3.1. USE OF XRMC

Before running XRMC, is necessary to define the input files that describe the experimental setup that you want to simulate. These files include a main input file, a

parameter file, and some device files. Device files contain the necessary parameters for the C ++ objects, used to perform the simulation. The main input file specifies the commands to load all device files, to execute the simulation, and to save the output file (GOLOSIO et al., 2013).

The typical configuration for X-ray imaging simulations or spectroscopy experiments includes the following device files (GOLOSIO et al., 2013):

- source device;
- spectrum device;
- detector device;
- sample device;
- composition device;
- quadricarray device;
- geom3d device (three-dimensional description of object geometry).

3.2. SAMPLE EXPLORATION SIMULATION METHODOLOGY

As shown in section 2 the process of scanning CT samples consists of producing x-rays of the interest object (in this case, sediment samples) from different angles, completing a full turn over the object. In our simulation one x-ray is produced for each rotation angle, totalizing 360 images for a complete rotation.

The XRMC software generates an image under the experiment specified conditions. Then to simulate the CT scanning process, is necessary to rotate the sample under analysis by running the simulation program for each set of input files. These input files represent the different positions (data collection angles) in which the object planes´ images must be produced. The methodology described is shown in figure 2.

The methodology execution, including the XRMC run and the input files update process was performed using a Linux shell script, that allows to perform these two processes at the same time. The modified input files were, the main file, to change the name of the next output file and the quadricarry file to rotate the studied object.
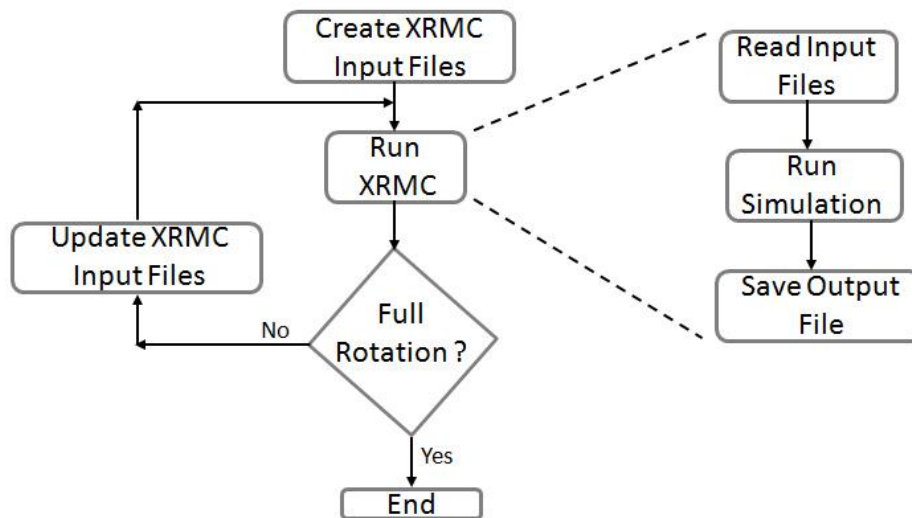
Figure 2. Flux diagram of the methodology to simulate CT samples exploration.

4. RESULTS

To represent the sediment layers in the XRMC, were simulated volumes with acetylene (C_2H_2) as Base Material (BM) and acetylene with 10% Barium ($C_2H_2$90% Ba10%) as Contrast Object (CO) (HOFF et al., 2017). The BM object was a cube with side varying from 10 to 50 cm, to evaluate the method. As COs, different geometric shapes were placed in the center of the cube. For samples with thicknesses up to 30 cm, a monochromatic photon beam of 30 keV was used. However, for samples with 30 to 50 cm thicknesses, were used a beam of photons of the Ir-192 spectra, generating satisfactory results.

Sediment imaging involves working with low contrast images. In initial tests, images with 8-bit color, and 256 gray tones were used, and the BM was a 10 cm side cube. In all simulations, the sample was placed in the center of the source-detector assembly. For 10 cm samples, the distance between the source and the detector was 40 cm. Figures 3 and 4 show an x-ray and a reconstruction plane for two COs, a 5 cm cube and a 2 cm radius sphere.

Observing the reconstructed images in Figures 3 and 4 we can notice that some artifacts emerge in the images. The visual analysis suggests reasonable quality images. Nevertheless, a more accurate analysis using automated macros in Fiji to compare the reconstructed volumes to the simulated volumes was unviable due to these artifacts and also the noise in the images.
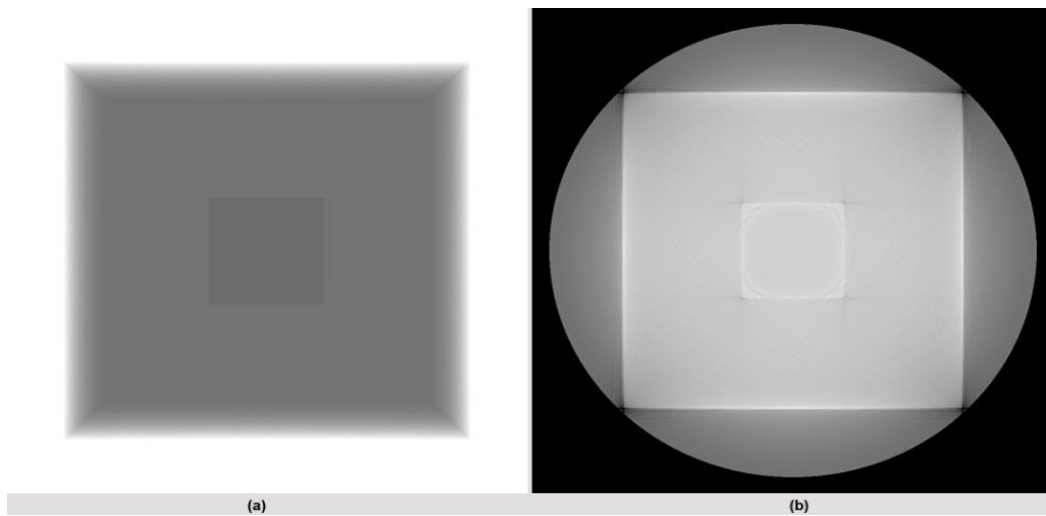
Figure 3. CO 5 cm cube, BM 10 cm cube, 8-bit colors. (a) Simulated radiograph for 0° observation angle, (b) central plane of the reconstruction.
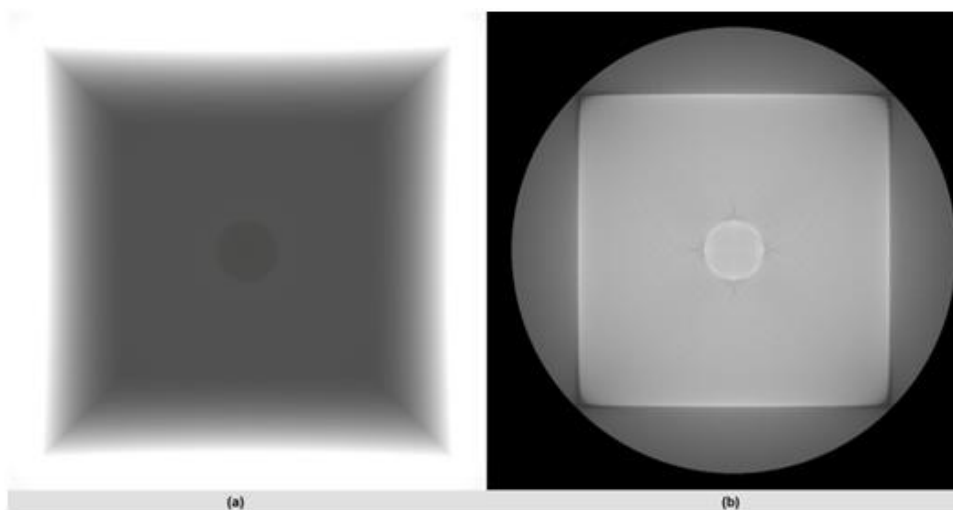

Figure 4. CO 2 cm radius sphere, MB 10 cm cube, 8-bit colors. (a) Simulated radiograph for 0° observation angle, (b) central plane of the reconstruction.

To overcome this problem, 64-bit color images were used, resulting in images with 1.8×10^{19} shades of gray. Figure 5 shows an X-ray and a reconstruction plane for a cubic OC of 5 cm side and a 10 cm side's cube of MB, using a 64-bit color images.

The x-ray in Figure 5 (a) represents appropriately the explored volume, even though, the low contrast between the BM and the OC in the image center difficult its detection visually. In Figure 5 (b), the reconstructed image, using 64-bit color, presents the same artifacts reported in the 256-grayscale images. However, in this case, the enhanced images and the noise reduction allow the automatic processing for statistical analysis.
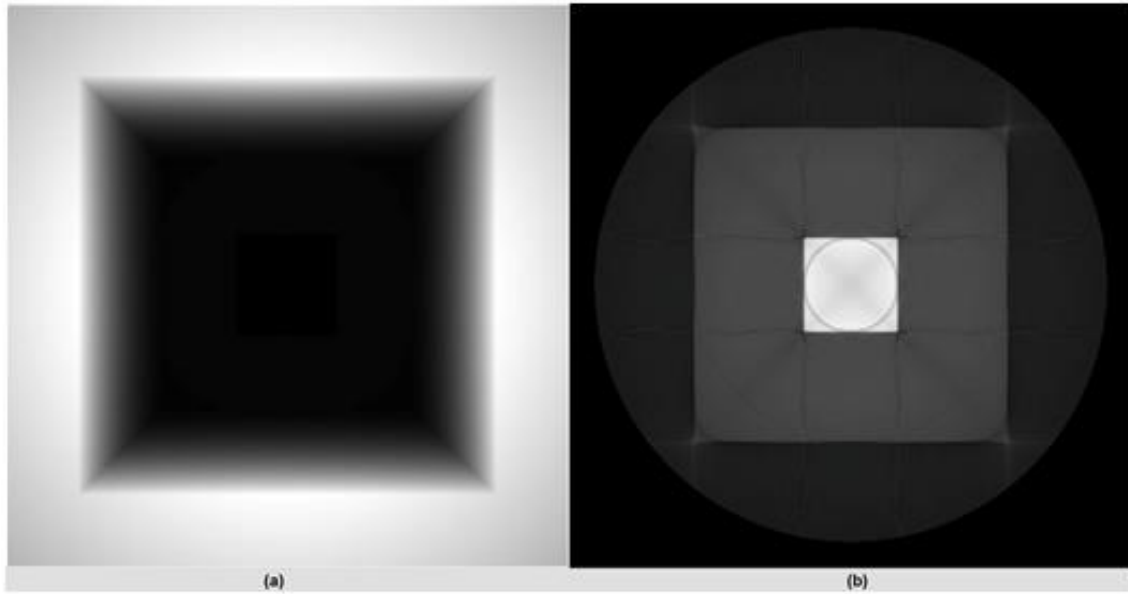
Figure 5. CO 5 cm cube, BM 10 cm cube, 64-bit colors. (a) Simulated radiograph for 0° observation angle, (b) central plane of the reconstruction.

Figures 6, 7, 8 and 9 show axial, sagittal and coronal planes of the reconstructed volumes center, for several COs with different dimensions' BMs using the 64-bit color images. The simulated COs were elliptical base cylinder and also, different layers varying its thicknesses and sizes. For samples of 30 cm side BMs the distance between the source and the detector was 100 cm and, for 50 cm side BMs this distance was 200 cm.
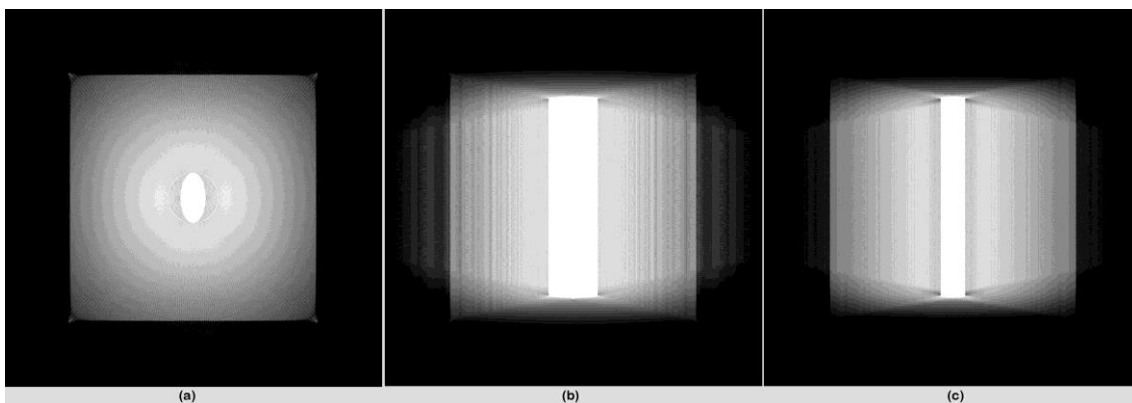

Figure 6. Reconstructed volume central planes for a cylindrical CO with BM 10 cm cube and 64-bit color images. (a) Axial plane, (b) sagittal plane and (c) coronal plane.
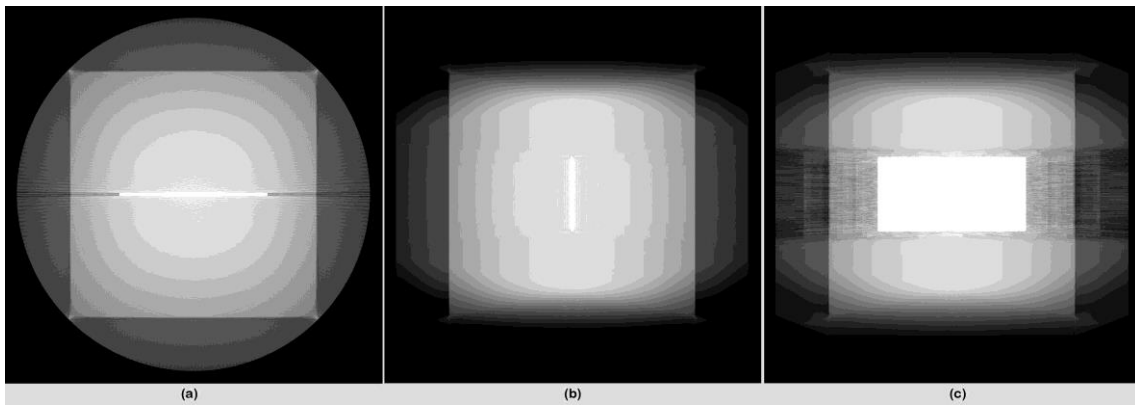
DOMINGUEZ, J.S; HOFF, G; DE ASSIS, J.T; BRUNETTI, A; IGLESIAS, S.M
3D reconstruction method applied to sediment layers in computed tomography geometry

Figure 7. Reconstructed volume central planes for a layer CO with BM 10 cm cube and 64-bit color images. (a) Axial plane, (b) sagittal plane and (c) coronal plane.
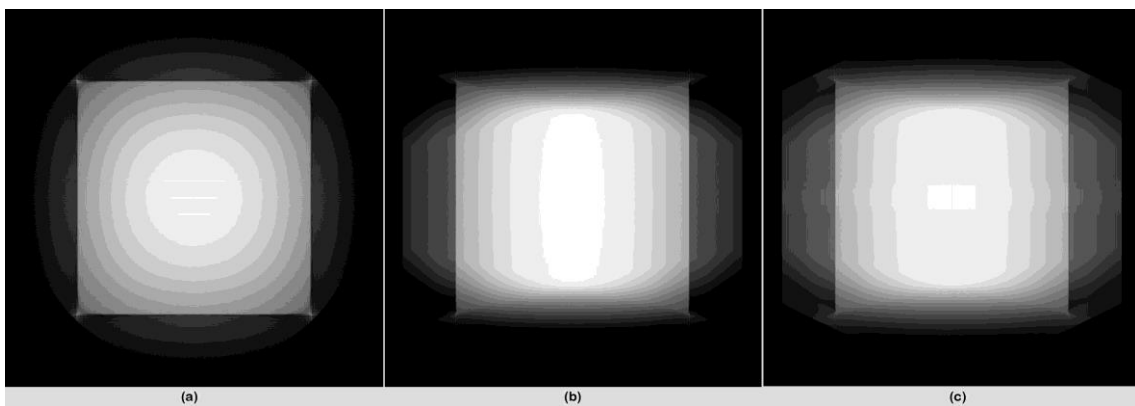

Figure 8. Reconstructed volume central planes for a three-layers CO with a BM 30 cm cube and 64-bit colors. Axial plane (a), sagittal plane (b), coronal plane (c).
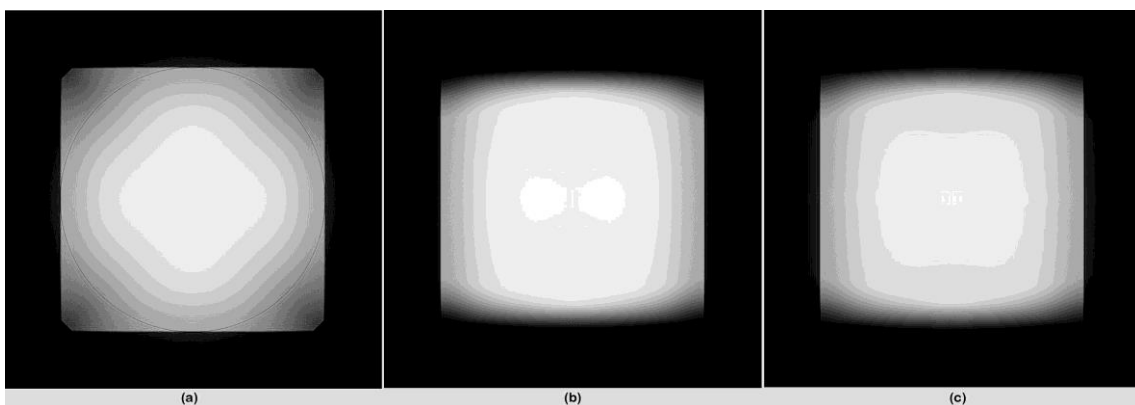

Figure 9. Reconstructed volume central planes for a layer CO with BM 50 cm cube and 64-bit color images. (a) Axial plane, (b) sagittal plane and (c) coronal plane.

In figures 6 and 7, is possible to observe that in the three planes the COs have well delimited edges without artifacts inside, and that several artifacts appear between the COs and the BM. In Figures 8 and 9 the COs edges are well delimited but a discontinuity appears

DOI: 10.18605/2175-7275/cereus.v13n3p68-82
Revista Cereus
2021 Vol. 13. N.3

DOMINGUEZ, J.S; HOFF, G; DE ASSIS, J.T; BRUNETTI, A; IGLESIAS, S.M
3D reconstruction method applied to sediment layers in computed tomography geometry

in the center of the layers in the coronal plane resulting from the signal intensity decreasing. Nevertheless, this artifact presence does not interfere in the automatic segmentation or CO measurement. Using automated macros in Fiji, a statistical comparison was performed between the simulated volumes (the expected object dimensions defined in the simulation) and the reconstructed volumes (the reconstructed objects' measured dimensions), obtaining errors less than 8%. The COs used on all samples had similar dimensions, the difference observed between the COs sizes in the figures 7, 8 and 9 are due to the different distances which detector were positioned to be able to irradiate the entire volumes.

In Figures 6 and 7 with smaller size samples and a lower energy beam the COs are most notable in the images. When the size and the energy beam increase in Figures 8 and 9, the contrast between the COs and the BMs decreases. Nevertheless, is still possible to differentiate the COs as a solid layer.

With these results, is possible to affirm, that the FDK algorithm was adequate to perform the samples 3D reconstruction considering the analyzed imaging, producing the axial images for the compared reconstructed volumes.

4.1. ARTIFACTS FOUND IN RECONSTRUCTED IMAGES

As can be noticed in the Figs (3-9), artifacts appear in all the reconstructed images dependents on the object's geometry and its edges. The reconstruction basis of the FDK algorithm is strongly linked with the object's edges, what is shown by the presence of these artifacts in our reconstructions. The fact of having low contrast images seems to reinforce this behavior. The mentioned artifacts are generated both in 8-bit color images, and in 64-bit color images, however there are more evident in the 64-bit images. Nevertheless, in 64-bit images, the signal intensity difference is greater in each region diminishing the artifacts interference. This factor, prevents low-resolution images automatic processing and does not jeopardize this process for high-resolution images.

It is important to point out, that the images were balanced (especially contrast and brightness) in order to highlight the artifacts, making them more evident for this discussion.

The artifacts associate with the edges and are generated inside the cube that forms the BM and also, inside and outside the COs. Figures 10 and 11 show, respectively, the artifacts in the cubic OCs slices for 8-bit and 64-bit color images. In figure 11 the artifacts appear sharper and are observed in larger quantity if compared with the figure 10. This is

due to the better image, nevertheless, a detailed analysis showed similar artifacts in both images. In the case of the cubic CO, the edges are located in the same positions for all the slices in which the cube is present, for that reason, similar artifacts appear in these slices. Regard the CO spherical geometry (figure 12) where the edges appear different in each slice, the artifacts also differ between the different slices. All of these artifacts are generated in a kind of ghost image where there is an object edge enhancement, but the signal strength remains constant. This type of artifact appears a few slices (from 3 to 5) before that a specific-material object appears and there are easily recognizable, if the contrast between the materials is considerable (that is, greater than the statistical fluctuation for each material signal).
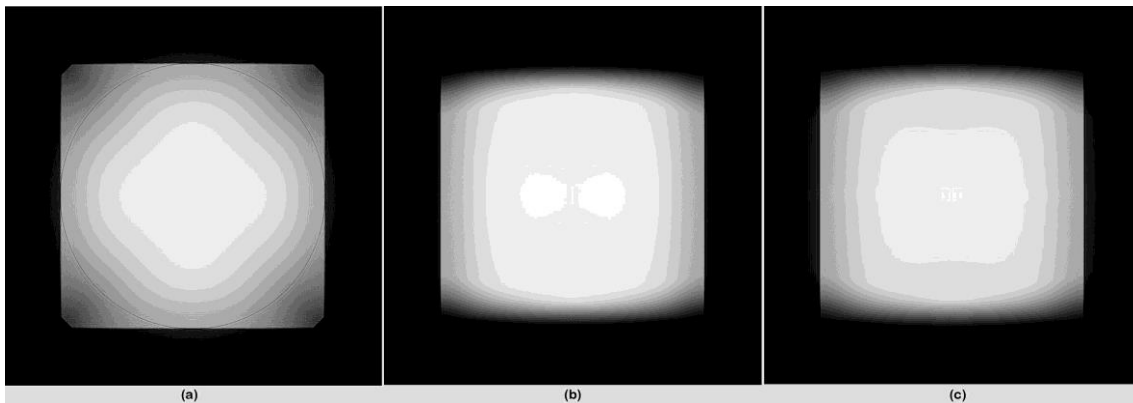

Figure 10. Artifacts in a cubic OC for an 8-bit color image. Artifacts at the edges of the outer cube (a), artifacts external to the OC (b), artifacts internal to the OC (c).
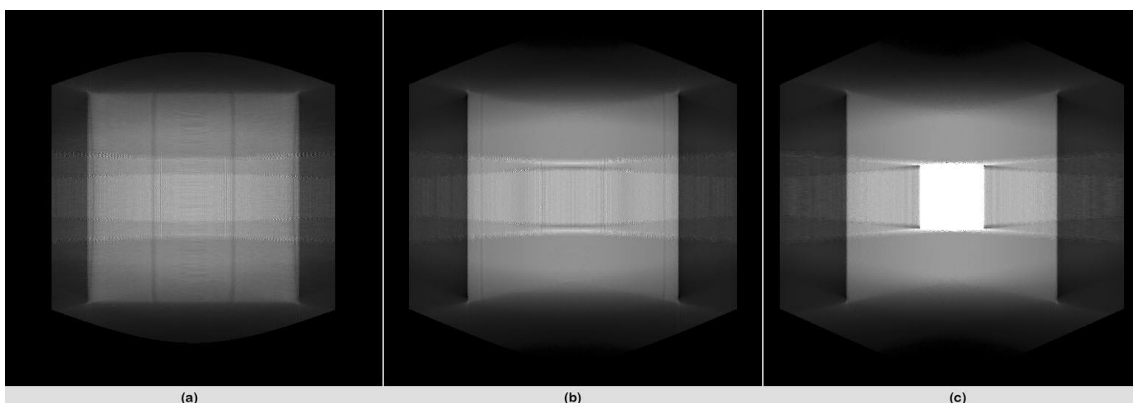

Figure 11. Artifacts in a cubic OC for a 64-bit color image. Artifacts at the edges of the outer cube (a), artifacts external to the OC (b), artifacts internal to the OC (c).

Figure 12 shows the identified artifacts for a sphere's CO. In Figure 12 (a) only the artifacts of the outer cube are observed, since the CO is far from the edge. In Figures 12 (b)

when the OC begin to appear and 12 (c) 40% the OC appears, the artifacts are different depending on the CO edges at different slices.
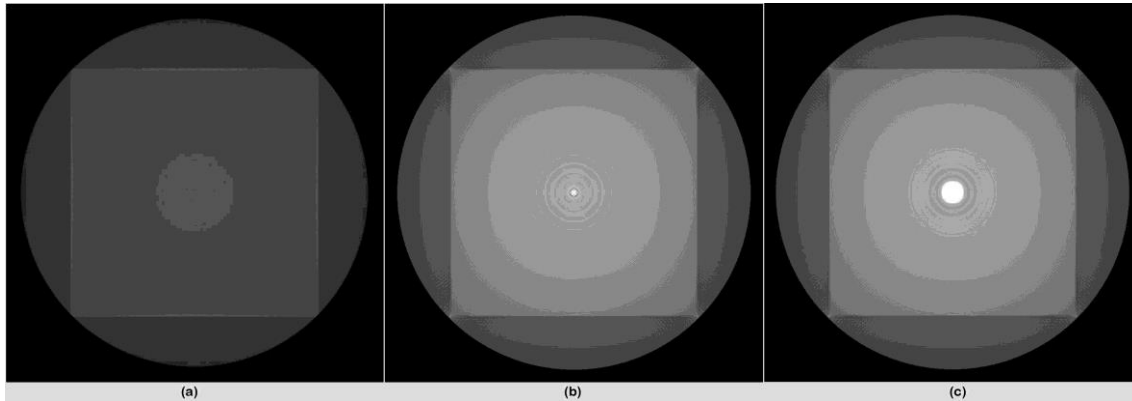

Figure 12. Artifacts in a spherical OC for 64-bit color. Artifacts at the edges of the outer cube (a), artifacts in the slices that begin to appear the OC (b), artifacts in the slices where 40% of the OC appears (c).

Comparing the images, especially Figures 11 and 12, the image object format influence on the generated artifacts is evident: straight lines or lines' rays for straight-side or with corners objects, and concentric circles for the circle objects case.

Figure 13 shows an artifact enlargement for the 1mm-layer OC. This enlargement improves the observation of the artifact structure and their dependence on the object's edges. In the original images the artifacts are noticed, but, their signal intensity is smaller if compared with the COs.

Figure 13. Enlargement of the spherical OC artifacts for 64-bit color image.

5. CONCLUSSIONS

This paper proposed a reconstruction method for computed tomography (CT) for obtaining images of the sediment deposition layers. To test the methodology, planar images of geometric objects in centered geometry, similar to those resulting from the CT processes, were simulated using the dedicated X-Ray Monte Carlo (XRMC) code. With these generated x-rays, using the Feldkamp, David and Kress (FDK) reconstruction algorithm three-dimensional volume were generated.

The results show that CT geometry or industrial radiography, with X-ray sources or Ir-192 seeds, are techniques that can be successfully applied to obtain sediment layers' images. The use of these techniques preserves the material integrity and produces images with information that would allow to locate or identify the several materials in the layers accurately.

This work demonstrates that, due to the possible low contrast between the elements present in this kind of samples, the images produced must be high quality to avoid their noise contamination or artifact's appearance in the image processing. The use of the FDK allows the method validation, however, as we analyze in section 4.1, this method produces numerous artifacts. Nevertheless, for images with 64-bit color, the images automatic processing is possible.

For future researches, the authors propose to evaluate pre and post processing techniques in order to reduce the artifacts' appearance in the reconstructed images as well as the testing other reconstruction algorithms for field use, with image recollection in defined solid angles.

REFERÊNCIAS

BJØRLIKKE, Knut. **Petroleum Geoscience: From Sedimentary Environments to Rock Physics**. Editora Springer, 2015

BRUNETTI, A.; DEPALMAS, A.; DI GENNARO, F.; SERGES, A. and SCHIAVON, N. X-ray fluorescence spectroscopy and Monte Carlo characterization of a unique nuragic artifact (Sardinia, Italy). **Spectrochimica Acta Part B: Atomic Spectroscopy,** Volume 121, 2016.

DOMINGUEZ, J. S. **Paralelização de algoritmos de reconstrução de imagens tomográficas usando unidades gráficas de processamento e processadores com múltiplos núcleos**. Tese (Doutorado em Modelagem Computacional) - IPRJ/UERJ, Nova Friburgo, 2016.

FELDKAMP, L. A.; DAVIS, L. C. and KRESS, J. W. Practical cone-beam algorithm. **J. Opt. Soc. Am**, v. 1, n. 6, 1984.

GOLOSIO, B.; SCHOOJANS, T.; BRUNETTI, A.; MASALA, G. L. and OLIVA, P. XRMC (X-ray Monte Carlo): version 6.4.1 TUTORIAL. Università degli Studi di Sassari, 2013.

GOLOSIO, B.; SCHOOKANS, T.; BRUNETI, A.; OLIVA, P. ans MASALA, G. L. Monte Carlo simulation of X-ray imaging and spectroscopy experiments using quadric geometry and variance reduction techniques. **Computer Physics Communications**, 2014.

HOFF, Gabriela; DE ASSIS, J. T.; BRUNETTI, A.; FANTI V.; and GOLOSIO, B. Abstract ID: 69 Validation of XRMC Monte Carlo toolkit for external dosimetry applied to mammography. **Physica Medica**. Volume 42, Supplement 1, 2017.

KALENDER, W.A. Computed Tomography: Fundamentals, System Technology, Image Quality, Applications. 3ª. **Erlangen: Publicis Publishing**, 2011.

MANSO, M.; SCHIAVON N.; QUERALT, I.; ARRUDA, A. M.; SAMPAIO J. M. and

BRUNETTI, A. Alloy characterization of a 7th Century BC archeological bronze vase — Overcoming patina constraints using Monte Carlo simulations. Spectrochimica Acta Part B: **Atomic Spectroscopy**, Volume 107, 2015.

MIALL, A. D. **The geology of fluvial deposits: sedimentary facies, basin analysis and petroleum geology.** Editora Springer, 2006.

OLIVA, P.; GOLOSIO, B.; MASALA, G.L.; SCHOOJANS, T.; BRUNETTI, A. and CARPINELLI, M. New Techniques in Diagnostic X-ray Imaging: A Simulation Tool and Experimental Findings. **Physics Procedia**. Volume 62, 2015.

OLIVEIRA, L. F. **Tomografia Computadorizada Tridimensional usando Raios-X na Análise de Objetos Volumétricos.** Tese (Doutorado em Engenharia Nuclear), COPPE/UFRJ, Rio de Janeiro, 2002.

SCHOOJANS, T. XRMC. 2017. Disponível em <https://github.com/golosio/xrmc/wiki>. Acesso junho 2018.

SHUNLI, Zang; GUOHUA, Geng and JIAN, Zhao. Fast parallel reconstruction for cone-beam FDK algorithm. Concurrency and Computation: Practice and Experience. **Wiley Online Library**, 2018.